Asymmetric Molecular Imaging through Decoding Odd-Even High-Order Harmonics

Y. J. Chen,[1] L. B. Fu,[2,3] and J. Liu[2,3]

[1]College of Physics and Information Technology, Shaanxi Normal University, Xi'an, China
[2]Institute of Applied Physics and Computational Mathematics, Beijing 100088, China
[3]Center for Applied Physics and Technology, Peking University, Beijing 100084, China

(Received 19 March 2013; published 12 August 2013)

The exquisite procedure for imaging a molecular orbital with high-order harmonics proposed by Itatani *et al.* [Nature (London) **432**, 867 (2004)] encounters difficulty when extended to an asymmetric molecule because the wave function there usually does not have a definite parity. With the observation that the wave function can be decomposed into a sum of odd and even functions and that the ionization process in harmonic generation is usually not sensitive to the asymmetry of the molecular potential, we predict that asymmetric molecular orbital imaging can be implemented through decoding odd-even high-order harmonics. A generalized tomography procedure is proposed, which has been certified by analytic deduction and numerical simulation. The above finding greatly extends the molecular tomography procedure and will further stimulate related experiments.

DOI: 10.1103/PhysRevLett.111.073902 PACS numbers: 42.65.Ky, 32.80.Rm

Introduction.—The tomographic imaging of molecular orbitals using high-order harmonic generation (HHG), which provides unprecedented access to the inner workings of molecules [1], is a timely topic and has stimulated great theoretical and experimental interest recently [2–6]. The molecular tomograph has potential applications in such fields as chemical reactions [7,8] and in tracing the electron dynamics in attosecond scales [9–11].

The molecular orbital–tomography procedure was first proposed by Itatani *et al.* for N_2 [12], and then extended to other molecules such as CO2 [13]. Recently, much attention has been paid to the asymmetric molecules of HeH^{2+} [14–16], CO [17–20], and HCl [21]. Because asymmetric molecules are widespread and important in chemical reactions, it is highly desired to probe their structure using current ultrafast laser facilities. However, the original orbital–tomography procedure encounters intrinsic difficulty because the wave function there usually does not have a definite parity [16]. To circumvent the dilemma thus requires unidirectional HHG recollision in the procedure [14,19], which nevertheless is not easy to manipulate in practical experiments.

In this Letter, we attempt to overcome the difficulty with decoding the odd-even high-order harmonics of asymmetric molecules. We show that in the tunneling regime, the emissions of odd (even) harmonics are closely related to the gerade (ungerade) component of the asymmetric highest occupied molecular orbital (HOMO). This observation allows us to generalize the orbital–tomography procedure to asymmetric molecules directly without the requirement of unidirectional recollision. With the generalized procedure, the asymmetric 5σ HOMO of the CO molecule is reconstructed successfully, as shown in Fig. 1. Our scheme can be applied to other complicated asymmetric linear molecules.

Generalized tomography procedure.—Let us first recall the tomography procedure proposed by Itatani *et al.* [12] for symmetric molecules. In the strong-field approximation (SFA) [22], the HHG intensity can be written as

$$S(\omega, \theta) = N^2(\theta)\omega^4 |a[k(\omega)]\mathbf{d}(\omega, \theta)|^2, \quad (1)$$

where $\mathbf{d}(\omega, \theta) = \langle \psi_0(\mathbf{r}, \theta)|\hat{\mathbf{r}}|k(\omega)\rangle$ is the transition dipole matrix element between the HOMO of $|\psi_0(\mathbf{r}, \theta)\rangle$, which is rotated by the Euler angle θ, and the continuum state $|k(\omega)\rangle$, which is described by a plane wave $|\exp[ik(\omega)x]\rangle$ with $k(\omega) = \sqrt{2\omega}$. $N(\theta)$ is the number of ions produced. $a[k(\omega)]$ is the complex amplitude of the continuum state $|k(\omega)\rangle$. It can be calibrated by a reference atom with a similar ionization potential I_p as the molecule (for CO, it is Kr). That is $|a[k(\omega)]| = \sqrt{S_a(\omega)}\omega^{-2}|\mathbf{d}_a(\omega)|^{-1}$. $S_a(\omega)$ and $\mathbf{d}_a(\omega)$ are the harmonic intensity and the dipole of the reference atom, respectively. Once $a[k(\omega)]$ is determined,

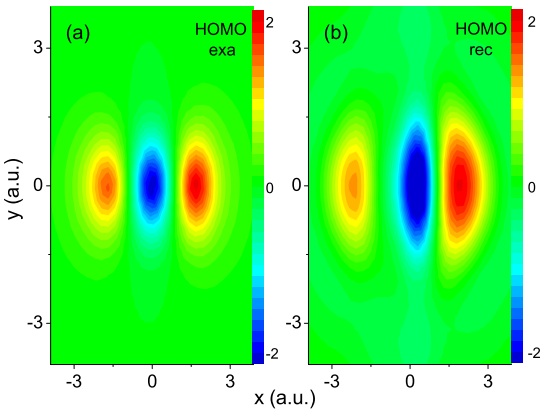

FIG. 1 (color online). Comparison of the exact (a) and the reconstructed (b) results for the 5σ HOMO wave function of the 3D model CO molecule projected in the xoy plane.

one can obtain the dipole $\mathbf{d}(\omega,\theta)$ of the symmetric molecule using Eq. (1). Because the HOMO of a symmetric molecule has gerade or ungerade parity, we can use $\mathbf{d}^g(\omega,\theta) = i\langle\psi_0^g(\mathbf{r},\theta)|\hat{\mathbf{r}}|\sin[k(\omega)x]\rangle$ for gerade cases or $\mathbf{d}^u(\omega,\theta) = \langle\psi_0^u(\mathbf{r},\theta)|\hat{\mathbf{r}}|\cos[k(\omega)x]\rangle$ for ungerade cases. The Fourier inversion of the dipole $\mathbf{d}^{g(u)}$ in the molecular frame is [11]

$$f_x^g(x,y) = i\sum_\theta\sum_\omega \sin[kq(\mathbf{r},\theta)][d_x^g\cos\theta + d_y^g\sin\theta],$$
$$f_y^g(x,y) = i\sum_\theta\sum_\omega \sin[kq(\mathbf{r},\theta)][d_y^g\cos\theta - d_x^g\sin\theta] \quad (2)$$

for gerade cases and

$$f_x^u(x,y) = \sum_\theta\sum_\omega \cos[kq(\mathbf{r},\theta)][d_x^u\cos\theta + d_y^u\sin\theta],$$
$$f_y^u(x,y) = \sum_\theta\sum_\omega \cos[kq(\mathbf{r},\theta)][d_y^u\cos\theta - d_x^u\sin\theta] \quad (3)$$

for ungerade cases with $q(\mathbf{r},\theta) = x\cos\theta + y\sin\theta$. ψ_0^g and ψ_0^u are obtained with $\psi_0^g = (f_x^g/x + f_y^g/y)/2$ and $\psi_0^u = (f_x^u/x + f_y^u/y)/2$.

For an asymmetric molecule, however, the HOMO of $\psi_0(\mathbf{r})$ does not have a definite parity. In this case, the dipole can be deduced from Eq. (1) only when unidirectional HHG recollision is ensured [14]. This requirement brings additional complexities into practical experiments. It is well known that the asymmetric wave function can be divided into gerade and ungerade parts with $\psi_0(\mathbf{r}) = \psi_0^g(\mathbf{r}) + \psi_0^u(\mathbf{r})$. Here, $\psi_0^{g(u)}(\mathbf{r}) = [\psi_0(\mathbf{r}) \pm \psi_0(-\mathbf{r})]/2$. Then the dipole moment of the asymmetric molecule can be written as $\mathbf{d}(\omega,\theta) = \mathbf{d}^g(\omega,\theta) + \mathbf{d}^u(\omega,\theta)$. Accordingly, Eq. (1) can be rewritten as

$$S(\omega,\theta) = N^2(\theta)\omega^4|a[k(\omega)][\mathbf{d}^g(\omega,\theta) + \mathbf{d}^u(\omega,\theta)]|^2. \quad (4)$$

According to the recent simulations for HeH^{2+} [16], the emission of odd (even) harmonics is mainly related to the dipole $\mathbf{d}^g$ ($\mathbf{d}^u$). With this observation, we have

$$S^{\text{odd}}(\omega,\theta) = N(\theta)\omega^4|a[k(\omega)]\mathbf{d}^g(\omega,\theta)|^2, \quad \omega = (2n+1)\omega_0,$$
$$S^{\text{even}}(\omega,\theta) = N(\theta)\omega^4|a[k(\omega)]\mathbf{d}^u(\omega,\theta)|^2, \quad \omega = 2n\omega_0. \quad (5)$$

Note that in Eq. (5) we have used $N(\theta)$ to replace $N^2(\theta)$ [3], since we are working in the case of a single molecule. Equation (5) reveals the qualitative relationship between the dipoles $\mathbf{d}^{g(u)}$ and spectra $S^{\text{odd(even)}}$.

Equation (5) can also be understood from the SFA [22]. According to the SFA, the product of the ionization $\mathbf{d}_i(t',t)$ and the recombination $\mathbf{d}_r(t',t)$ dipole moments parallel to the laser polarization that is along the x direction is $d_{ix}d_{rx} = \langle k_{ix}|x|\psi_0\rangle\langle\psi_0|x|k_{rx}\rangle = d_{ix}^g d_{rx}^g + d_{ix}^u d_{rx}^u + d_{ix}^g d_{rx}^u + d_{ix}^u d_{rx}^g$ with $d_{ix}^{g(u)} = \langle k_{ix}|x|\psi_0^{g(u)}\rangle$, $d_{rx}^{g(u)} = \langle\psi_0^{g(u)}|x|k_{rx}\rangle$, and $|\psi_0(\mathbf{r},\theta)\rangle = |\psi_0^g(\mathbf{r},\theta)\rangle + |\psi_0^u(\mathbf{r},\theta)\rangle$. $k_{ix} \equiv k_{ix}(t',t)$ is the instantaneous velocity of the electron along the field direction at the ionization time t' and $k_{rx} \equiv k_{rx}(t',t)$ is that at the recombination time t. Because of the symmetry of ψ_0^g and ψ_0^u, the terms $d_{ix}^{g(u)}d_{rx}^{g(u)}$ representing that the electron ionizes from and returns to the same components of ψ_0 contribute to odd harmonics, whereas the terms $d_{ix}^{g(u)}d_{rx}^{u(g)}$ relating to different components contribute to even ones. As shown in Ref. [16], due to tunneling, the continuum electron wave packet generated from an asymmetric molecule is similar to the symmetric one with the same I_p. These imply that only the ionization dipole d_{ix}^g relating to the main component ψ_0^g of the asymmetric HOMO (such as the 5σ orbital for CO) contributes significantly to ionization. Accordingly, only the term $d_{ix}^g d_{rx}^g$ ($d_{ix}^g d_{rx}^u$) contributes significantly to odd (even) harmonics, in agreement with Eq. (5). Since the main contributions to odd and even harmonics come from the same ionization dipole d_{ix}^g, their spectral amplitudes are also similar. One can evaluate the spectral amplitude of even harmonic $2n\omega_0$ using $a[k(2n\omega_0)] = \{a[k((2n+1)\omega_0)] + a[k((2n-1)\omega_0)]\}/2$.

Once $|\mathbf{d}^g|$ and $|\mathbf{d}^u|$ are determined from Eq. (5), and their signs are judged using the harmonic phase [11,13], or alternatively, using the interference minimum in the spectrum [12,14], by virtue of Eqs. (2) and (3) one can obtain $\psi_0^g(x,y)$ and $\psi_0^u(x,y)$. Then the asymmetric HOMO $\psi_0(x,y) = \psi_0^g(x,y) + \psi_0^u(x,y)$ can be obtained.

Application.—As an illustration, in the following, we will apply the above procedure to the reconstruction of the 5σ HOMO for the CO molecule.

(i) CO model:—To simulate the dynamics of the CO molecule in strong laser fields, we use a single-active-electron model. We assume that the molecular axis is located in the xoy plane with an angle θ to the x axis and the direction of the electric field $\mathbf{E}(t)$ is along the x axis. The Hamiltonian is $H(t) = \mathbf{p}^2/2 + V(\mathbf{r}) + \mathbf{r}\cdot\mathbf{E}(t)$ (in atomic units) with the soft-core potential [23]

$$V(\mathbf{r}) = -\sum_{j=1,2}\frac{(Z_{ji} - Z_{jo})\exp(-\mathbf{r}_j^2/\rho) + Z_{jo}}{\sqrt{\xi + \mathbf{r}_j^2}}, \quad (6)$$

where Z_1 and Z_2 are the screened effective nuclear charges for the O center and the C center, respectively. The indices i and o denote the inner and outer limits of Z_1 and Z_2. ξ and ρ are the softening and the screening parameters with $\xi > 0$ and $\rho > 0$. $\mathbf{r}_j = \mathbf{r} - \mathbf{R}_j$ with $\mathbf{R}_1$ and $\mathbf{R}_2$ being the positions of the nuclei that have the coordinates (x_1, y_1) and (x_2, y_2) in the xoy plane. $x_{1/2} = \pm R_{1/2}\cos\theta$, $y_{1/2} = \pm R_{1/2}\sin\theta$, $R_1 = R/(1+\beta)$, and $R_2 = \beta R/(1+\beta)$ with $\beta = Z_1/Z_2$. $R = 2.13$ a.u. is the internuclear separation. Here, following Ref. [23], we use the parameters of $Z_{1i} = 6$, $Z_{2i} = 4$, $Z_{1o} = 0.6$, and $Z_{2o} = 0.4$ with $\beta = Z_{1i}/Z_{2i} = Z_{1o}/Z_{2o}$ for CO. We adjust the other parameters ξ and ρ such that the ionization potential of the lowest state, corresponding to the 5σ symmetry, matches the CO value of 14 eV. This state, obtained through

imaginary-time propagation, is chosen as the initial state in the propagation of the time-dependent Schrödinger equation (TDSE) of $i\dot{\Psi}(t) = H(t)\Psi(t)$. The electric field used here is $\mathbf{E}(t) = \vec{\mathbf{e}}_x E \sin\omega_0 t$. $\vec{\mathbf{e}}_x$ is the unit vector along the x axis. We use a ten-cycle laser pulse, which is linearly ramped up for three optical cycles and then kept at constant intensity for seven additional cycles. With the relatively long pulse, the asymmetric ionization [15] basically plays no role in HHG. To minimize the multiphoton effect, as in Ref. [13], we work at the long laser wavelength of $\lambda = 1500$ nm with $I = 1 \times 10^{14}$ W/cm^2. We solve the TDSE numerically using the spectral method [24] with 4096 time steps per optical cycle. In 2D cases, $\xi = 0.5$ and $\rho = 1.746$ with a grid size of 410×102 a.u. for the x and y axes are used. In 3D cases, they are $\xi = 0.5$ and $\rho = 0.805$ with $410 \times 102 \times 51$ a.u. for the x, y, and z axes. In our simulations, the 2D reconstruction (see Fig. 4) is similar to the 3D one in Fig. 1 but shows stronger asymmetry due to the lower degrees of freedom. Below, we will introduce the generalized procedure in detail and focus our discussions on 2D cases for simplicity.

(ii) HHG spectra:—Some typical spectra emitted along the laser polarization for the model CO molecule are presented in the first row of Fig. 2. For comparison, we have plotted the odd and even harmonics using solid and dotted curves, respectively. Moreover, the harmonic yields at the angle θ have been divided by the ionization yields $N(\theta)$, which are evaluated using $N(\theta) = 1 - \langle\Psi(t) \mid \Psi(t)\rangle$ at the end of the pulse. In our simulations, the yields decrease as the angle θ increases and $N(\theta = 0°)$ is 2 orders of magnitude higher than $N(\theta = 90°)$.

These HHG spectra in Fig. 2 present two main characteristics: (1) the odd spectra show a broad hollow, the position of which shifts towards higher harmonic orders with the increase of the angle, as indicated by the dashed arrows. (2) The even spectra are comparable with the odd ones only in the hollow region. They decrease as the angle increases and disappear at $\theta = 90°$ (not shown here).

A deep insight into the relation between structure and HHG can be obtained as we further compare the odd versus even HHG spectra to the relevant dipoles $\mathbf{d}^g$ versus $\mathbf{d}^u$. As shown in the second row of Fig. 2, the behaviors of the dipole curves of $\mathbf{d}^g$ and $\mathbf{d}^u$, obtained with the exact 5σ wave function ψ_0 (TDSE initial state) and using the expressions shown just above Eq. (2), agree with the corresponding odd versus even spectra. For every case of angle θ in Fig. 2, one can see the broad hollow with a sharp minimum arising from intramolecular interference [16,25] in the $\mathbf{d}^g$ (solid) curve, as in the odd spectrum. When lower than the solid one on the whole, the $\mathbf{d}^u$ (dashed) curve manifests itself in the hollow region.

The close relation between the relevant dipoles and spectra can also be seen in Fig. 3. For two different angles, the $\mathbf{d}^g$ curves in the lower panels show a clear intersection [4]. The minima in the two curves are located at either side of this intersection point. This intersection phenomenon can also be found in the corresponding spectra in the higher panels, as indicated by the dashed arrows. Around the intersection, the relative yields of harmonics at two different angles change sign. These comparisons support our previous analyses. They tell us that odd (even) harmonics are mainly related to the gerade (ungerade) component of the asymmetric HOMO.

(iii) Reconstructed HOMO:—Using the generalized procedure, we have reconstructed the gerade $\psi_0^g(x, y)$ and ungerade $\psi_0^u(x, y)$ components of the 5σ wave function $\psi_0(x, y)$. In this reconstruction, (1) the molecular dipoles $\mid \mathbf{d}^g \mid$ and $\mid \mathbf{d}^u \mid$ are extracted from the ionization and HHG data calculated between 0° and 90° with a step of $\triangle\theta = 5°$ using Eq. (5). The dipoles at other angles are extrapolated by imposing the assumed symmetry related to the 5σ orbital to be imaged [11]. (2) A reference atom, which is

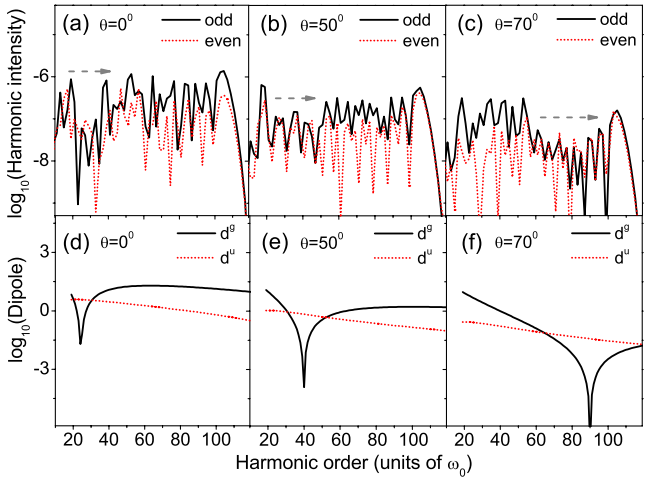

FIG. 2 (color online). Odd (even) harmonic spectra (a)–(c) versus the relevant dipoles $|\vec{\mathbf{e}}_x \cdot \mathbf{d}^{g(u)}(\omega, \theta)|^2$ (d)–(f) of the 2D model CO molecule for different orientation angles θ.

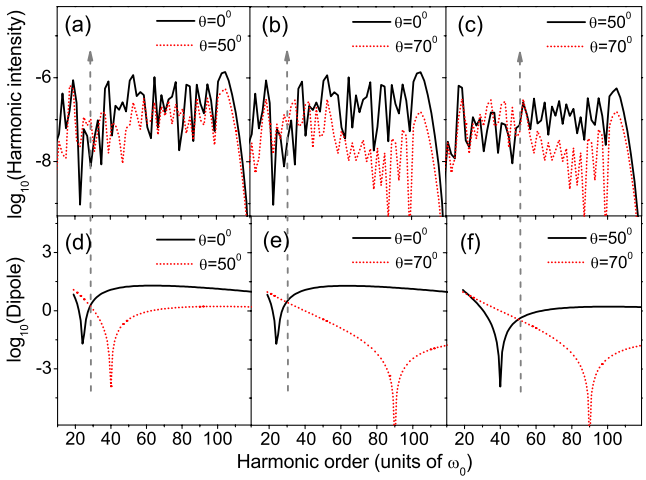

FIG. 3 (color online). Comparison of odd harmonic spectra (a)–(c) and the relevant dipoles $|\vec{\mathbf{e}}_x \cdot \mathbf{d}^g(\omega, \theta)|^2$ (d)–(f) of the 2D model CO molecule for different orientation angles θ.

modeled still using the potential Eq. (6) and is initially in an eigenstate with $2s$ symmetry, has been used instead of the Kr atom with a $4p$ valence orbital. Since at present we have inadequate knowledge of the effective potential working for Kr. (3) Only the contribution of the harmonics parallel to the laser polarization is considered [11,14]. Our further simulations show that the inclusion of the perpendicular harmonics in the present case does not improve the agreement between the reconstructed and the exact results on the whole. (4) Because the harmonic phase for asymmetric molecules is easily subject to the Stark effect [20], we use the interference minimum to identify the sign of the dipole [12]. Specifically, the minimum in the broad hollow of the odd spectrum, as seen in Fig. 2, can be used to judge the sign of the $\mathbf{d}^g$ dipole [25]. The even spectra do not show a broad hollow and differ mainly at a vertical scaling factor for different angles. These imply that the $\mathbf{d}^u$ dipole does not change sign in the spectral region explored here. In some cases, the minimum cannot be easily read directly from the spectrum. However, it can be identified as we compare the spectrum at angle θ_1 to that at θ_2. The minimum basically corresponds to the harmonic order at which the relative yields of harmonics at θ_1 and θ_2 go through their maximum, as shown in Fig. 3.

The reconstructions, shown in Figs. 4(d) and 4(e), are comparable with the exact ones showing $3\sigma_g$ and $2\sigma_u$ symmetries in Figs. 4(a) and 4(b), especially for the gerade component $3\sigma_g$ $\psi_0^g(x, y)$. For the ungerade component $2\sigma_u$ $\psi_0^u(x, y)$, the two central lobes near the y axis are striking in Fig. 4(e), as they have small amplitudes in Fig. 4(b). This disagreement arises from the orbital nodes of $2\sigma_u$ $\psi_0^u(x, y)$ at $x = 0$, which will induce numerical singularities in the length-form tomography procedure. To avoid a similar numerical question in orbital reconstruction with $1\pi^u$ symmetry, Haessler *et al.* [11] used the velocity form of the dipole. But for $3\sigma_g$ symmetry, their simulations also show that the length-form dipole works better. Here, we need to evaluate 5σ ψ_0 using $\psi_0 = \psi_0^g + \psi_0^u$. For consistency, we work with the length-form dipole in all cases and treat this singularity simply through evaluating $\psi_0^u(x, y)$ at $x^2 + y^2 \neq 0$.

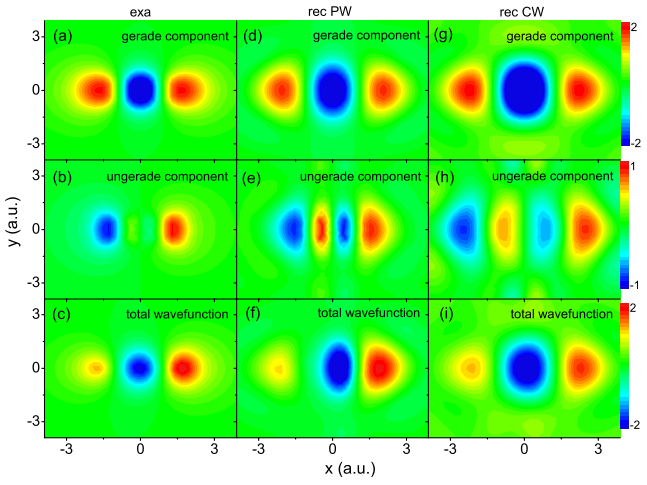

FIG. 4 (color online). Comparison of the exact results (left column), the reconstructions with plane waves (middle column), and Coulomb waves (right column) for ψ_0^g (first row), ψ_0^u (second row), and ψ_0 (third row) of 5σ wave function of the 2D model CO molecule.

The total reconstructed wave function ψ_0 is presented in Fig. 4(f). It holds the main characteristic of the exact one (TDSE initial state) in Fig. 4(c), which shows three main lobes with alternating signs and weights, separated by two nodal surfaces passing through each nucleus. The remaining deviation is that the separations between these three lobes are somewhat larger in Fig. 4(f) than in Fig. 4(c). This can arise from the inaccurate position of the interference minimum read from the HHG data in this reconstruction. The minimum can be influenced by the contributions from other HHG channels that are not included in Eq. (5). This deviation can also arise from the orbital nodes of $2\sigma_u$ $\psi_0^u(x, y)$, as discussed above.

(iv) Orientation and Coulomb effects:—Above, for simplicity, we have introduced the generalized procedure with the assumption of perfect orientation as well as continuum states described using plane waves (PW). For the case of incomplete orientation, our extended simulations show that when the degree of orientation $\langle\cos\theta\rangle$ is close to 0.25 (assuming perfect alignment), the asymmetry of the 5σ orbital can still be read from the reconstruction using the proposed procedure (see the Supplemental Material [26]).

We also extend to take into account the parent ion field in the recombination process using Coulomb waves (CW) instead of PW [11]. The results are shown in Figs. 4(g)–4(i), which are similar to the plane-wave-based ones in Figs. 4(d)–4(f), especially for the gerade component and the total wave function (see the Supplemental Material [26]). The CW result in Fig. 4(h) for the ungerade component shows a smaller amplitude for the two central lobes near the y axis but a somewhat larger size compared to the PW result in Fig. 4(e). The latter phenomenon was also observed in Ref. [11] for reconstructing the π_u orbital and is expected to be related to the orbital nodes of σ_u symmetry. As discussed in Ref. [27], the precision of the reconstruction is mainly limited by the accessible HHG spectral region. We thus expect that with the use of a long laser wavelength (1500 nm) and accordingly a broad accessible HHG spectral range ($0.6 \leq \omega \leq 3.2$ a.u., the influence of the Coulomb effect will not be so remarkable here.

In summary, we have investigated the HOMO reconstruction for the asymmetric molecule CO using a generalized HHG tomography procedure. Our procedure is applicable to other asymmetric linear molecules. For complicated top molecules, due to the absence of cylindrical symmetry, retrieving a complete tomographic image in principle requires probing the molecule from all

orientations. Since asymmetric molecules are active in many chemical processes, our results have important implications for probing the structure and dynamics of asymmetric molecules in ultrafast processes.

Very recently, Frumker and co-workers reported their experimental results for orienting the polar molecule CO in an intense pulse [28]. One would therefore expect to achieve orbital tomography of asymmetric molecules in experiments with the proposed procedure.

This work was supported by CAEP Foundation Project No. 2011B0102031, NFRP Grant No. 2013CB834100, NNSF Grants No. 11274090 and No. 11274051.

[1] P. B. Corkum, Phys. Rev. Lett. **71**, 1994 (1993).
[2] S. Patchkovskii, Z. X. Zhao, T. Brabec, and D. M. Villeneuve, Phys. Rev. Lett. **97**, 123003 (2006).
[3] Van-Hoang Le, Anh-Thu Le, Rui-Hua Xie, and C. D. Lin, Phys. Rev. A **76**, 013414 (2007).
[4] Y. J. Chen, J. Liu, and Bambi Hu, J. Chem. Phys. **130**, 044311 (2009).
[5] B. K. McFarland, J. P. Farrell, P. H. Bucksbaum, and M. Ghr, Science **322**, 1232 (2008).
[6] D. Shafir, Y. Mairesse, D. M. Villeneuve, P. B. Corkum, and N. Dudovich, Nat. Phys. **5**, 412 (2009).
[7] H. J. Wörner, J. B. Bertrand, D. V. Kartashov, P. B. Corkum, and D. M. Villeneuve, Nature (London) **466**, 604 (2010).
[8] P. Hockett, C. Z. Bisgaard, O. J. Clarkin, and A. Stolow, Nat. Phys. **7**, 612 (2011).
[9] P. B. Corkum and F. Krausz, Nat. Phys. **3**, 381 (2007).
[10] O. Smirnova, Y. Mairesse, S. Patchkovskii, N. Dudovich, D. Villeneuve, P. Corkum, and M. Yu. Ivanov, Nature (London) **460**, 972 (2009).
[11] S. Haessler, J. Caillat, W. Boutu, C. Giovanetti-Teixeira, T. Ruchon, T. Auguste, Z. Diveki, P. Breger, A. Maquet, B. Carré, R. Taïeb, and P. Salières, Nat. Phys. **6**, 200 (2010).
[12] J. Itatani, J. Levesque, D. Zeidler, H. Niikura, H. Pepin, J. C. Kieffer, P. B. Corkum, and D. M. Villeneuve, Nature (London) **432**, 867 (2004).
[13] C. Vozzi, M. Negro, F. Calegari, G. Sansone, M. Nisoli, S. De Silvestri, and S. Stagira, Nat. Phys. **7**, 822 (2011).
[14] E. V. van der Zwan, C. C. Chirila, and M. Lein, Phys. Rev. A **78**, 033410 (2008).
[15] Xue-Bin Bian and A. D. Bandrauk, Phys. Rev. Lett. **105**, 093903 (2010).
[16] Y. J. Chen and B. Zhang, Phys. Rev. A **84**, 053402 (2011).
[17] H. Li, D. Ray, S. De, I. Znakovskaya, W. Cao, G. Laurent, Z. Wang, M. F. Kling, A. T. Le, and C. L. Cocke, Phys. Rev. A **84**, 043429 (2011).
[18] E. Hasovic, M. Busuladzic, W. Becker, and D. B. Milosevic, Phys. Rev. A **84**, 063418 (2011).
[19] M. Y. Qin, X. S. Zhu, Q. B. Zhang, and P. X. Lu, Opt. Lett. **37**, 5208 (2012).
[20] A. Etches, M. B. Gaarde, and L. B. Madsen, Phys. Rev. A **86**, 023818 (2012).
[21] H. Akagi, T. Otobe, A. Staudte, A. Shiner, F. Turner, R. Dörner, D. M. Villeneuve, and P. B. Corkum, Science **325**, 1364 (2009).
[22] M. Lewenstein, Ph. Balcou, M. Yu. Ivanov, A. L'Huillier, and P. B. Corkum, Phys. Rev. A **49**, 2117 (1994).
[23] R. de Nalda, E. Heesel, M. Lein, N. Hay, R. Velotta, E. Springate, M. Castillejo, and J. P. Marangos, Phys. Rev. A **69**, 031804(R) (2004).
[24] M. D. Feit, J. A. Fleck, Jr., and A. Steiger, J. Comput. Phys. **47**, 412 (1982).
[25] M. Lein, N. Hay, R. Velotta, J. P. Marangos, and P. L. Knight, Phys. Rev. Lett. **88**, 183903 (2002).
[26] See Supplemental Material at http://link.aps.org/supplemental/10.1103/PhysRevLett.111.073902 for more details.
[27] P. Salières, A. Maquet, S. Haessler, J. Caillat, and R. Taïeb, Rep. Prog. Phys. **75**, 062401 (2012).
[28] E. Frumker, C. T. Hebeisen, N. Kajumba, J. B. Bertrand, H. J. Wörner, M. Spanner, D. M. Villeneuve, A. Naumov, and P. B. Corkum, Phys. Rev. Lett. **109**, 113901 (2012).